A ZERO-VOLTAGE SWITCHED PWM BOOST CONVERTER WITH AN ENERGY FEEDFORWARD AUXILIARY CIRCUIT

Gerry Moschopoulos, Praveen Jain, Yan-Fei Liu* and Geza Joos

Concordia University
Department of Electrical & Computer Engineering
P. D. Ziogas Laboratory
1455 de Maisonneuve Blvd. West
Montreal, Quebec, Canada, H3G 1M8
Tel. (514) 848-3116
Fax (514) 848-2802

*Nortel Technologies
P.O. Box 3511, Station C
Ottawa, Ontario, Canada, K1Y 4H7
Tel. (613) 763-3937
Fax. (613) 763-7155

Abstract- A zero-voltage switched (ZVS) PWM boost converter with an energy feedforward auxiliary circuit is proposed in this paper. This converter can be operated with PWM control because ZVS operation is achieved with an auxiliary resonant circuit that has few switching losses and handles much less power than the main power circuit as it is activated for only a small fraction of the switching cycle. Moreover, peak switch stresses are lower than those found in other proposed converters because some of the energy circulating in the auxiliary circuit is fed to the load. In the paper, the modes of converter operation are explained and analyzed, design guidelines are given, and experimental results are presented.

I. INTRODUCTION

The pulsewidth modulated (PWM) boost converter is widely used as a dc-dc converter and as a high power factor preregulator for power supplies. While the boost converter works well in these applications, the switching losses of the boost switch and the reverse recovery characteristic of the boost diode have a negative impact on its operation. The switching losses of the boost switch, which consist of turn-on and turn-off losses, create a significant amount of power dissipation. Consequently, large heat sinks must be added to the converter or the switching frequency must be limited to a low value, but these measures increase the size of the converter.

The reverse recovery characteristic of the boost diode causes the diode to experience reverse current through it as stored charge is being removed. This causes the switch current to have a high, sharp peak and increases EMI - especially if the diode is a fast-recovery diode which turns off abruptly. Solutions such as using a slow recovery diode, slowing down the turn-on of the boost switch and using passive snubbers are commonly used in conventional PWM boost converters to deal with these problems, but they introduce other losses which reduce efficiency and limit converter switching frequency.

Several boost converters [1] - [6] have been proposed in recent years, to try to overcome the problems of switching losses and diode reverse recovery. These converters, generally classified as zero-voltage-transition (ZVT) converters, have an auxiliary resonant circuit that is used to ensure that the boost diode has a soft turn-off and the main boost switch is turned on under zero-voltage switching (ZVS) conditions. Since the auxiliary circuit is in operation only when current is being transferred from the boost diode to the main switch, these converters behave exactly like PWM converters for most of the switching cycle. ZVT converters that have been proposed in the literature, however, have at least one of the following drawbacks:

(1) Soft-switching of the main switch is achieved by using an auxiliary switch that does not have a lossless turn-off.
(2) A dissipative snubber must be used to minimize oscillations that are caused by the interaction of an auxiliary circuit inductor with the output capacitance of the auxiliary switch.
(3) The converter switches have very high voltage stresses and/or very high peak current stresses. In some proposed converters these stresses can exceed twice the stresses found in standard PWM boost converters.

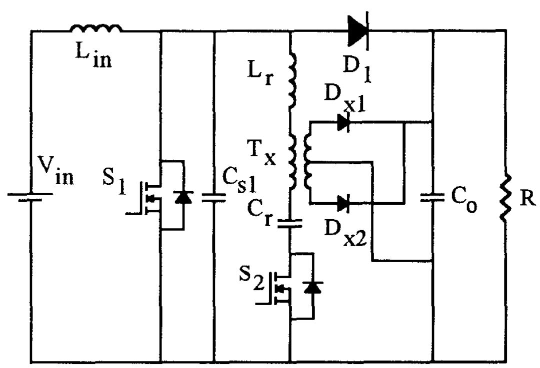

Fig. 1. The proposed ZVS PWM boost converter.

0-7803-3500-7/96/$ 5.00 © 1996 IEEE

(4) The auxiliary circuit is not simple.
(5) A floating gate drive is required for the auxiliary switch because it is not connected to ground.
(6) The converter cannot be used in PFC applications.

A ZVS PWM boost converter that does not have the above-mentioned drawbacks is proposed in this paper. This converter, shown in Fig. 1, achieves ZVS operation with a simple auxiliary resonant circuit that is connected parallel to the main switch and has few switching losses. Although the operation of the auxiliary circuit does cause the main switch to operate with a resonant current peak, this peak is much lower than that found in other proposed converters because some of the energy circulating in the auxiliary circuit is fed to the load by the transformer T_X. In the paper, the modes of operation of the converter are explained and analyzed, guidelines for the selection of the converter components are given and experimental results are presented.

II Modes Of Operation

In this section, the various modes of converter operation are explained and shown in Figs. 2 and 3, and a mathematical analysis of each mode of operation is given. This analysis is based on the following assumptions:

(1) The input inductor, L_{in}, is large enough to be considered as a constant current source, I_{in}, during the time that current is flowing through the auxiliary circuit.
(2) The output filter capacitor, C_0, is large enough to be considered as a voltage source, V_0.
(3) The auxiliary switch, S_2, has a resistance of R_r when it is turned on.
(4) The main switch, S_1, has a negligible resistance.
(5) The transformer, T_X, acts as a voltage source V_X when current is flowing in the auxiliary circuit. The polarity of V_X is dependent on the polarity of the auxiliary circuit current.

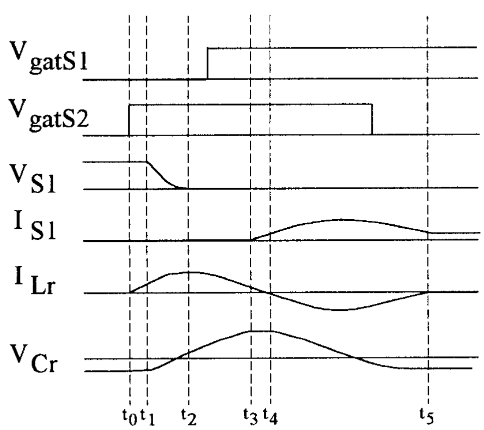

Fig. 2. Waveforms of the auxiliary resonant circuit.

(a) *Mode 0* [$t < t_0$]: The main switch, S_1, and the auxiliary switch, S_2, are both off, and current is flowing to the load through diode D_1. The auxiliary circuit capacitor, C_r, is charged to a voltage, V^*, which is negative. The voltage across the auxiliary switch is equal to $V_0 - V^*$.

(b) *Mode 1* [t_0- t_1]: The auxiliary switch S_2 is turned on under ZCS conditions as the resonant inductor L_r limits the di/dt. Current is diverted from diode D_1 as the current flowing through the auxiliary circuit rises. The state equations for this mode are:

$$L_r \frac{dI_{Lr}}{dt} = V_o - V_x - \frac{1}{C_r}\int_0^t I_{Lr}\, dt - V^* - I_{Lr}R_r \qquad (1)$$

$$C_r \frac{dV_{Cr}}{dt} = I_{Lr}\,. \qquad (2)$$

The state variables are the current flowing through the auxiliary circuit inductor, I_{Lr}, and the voltage across the auxiliary circuit capacitor, V_{Cr}. Using the initial conditions $I_{Lr} = 0$, and $V_{Cr} = V^*$, equ. (1) and (2) can be solved to give:

$$I_{Lr} = \frac{V_o - V_x - V^*}{\omega_r L_r} e^{-\xi t} \sin\omega_r t \qquad (3)$$

$$V_{Cr} = V_o - V_x - \frac{\omega_o}{\omega_r}(V_o - V_x - V^*)e^{-\xi t}\cos(\omega_r t - \psi) \qquad (4)$$

where

$$\xi = \frac{R_r}{2L_r} \qquad (5) \qquad\qquad \omega_r = \sqrt{\omega_o^2 - \xi^2} \qquad (7)$$

$$\omega_o = \frac{1}{\sqrt{L_r C_r}} \qquad (6) \qquad\qquad \psi = \tan^{-1}\frac{\xi}{\omega_r}. \qquad (8)$$

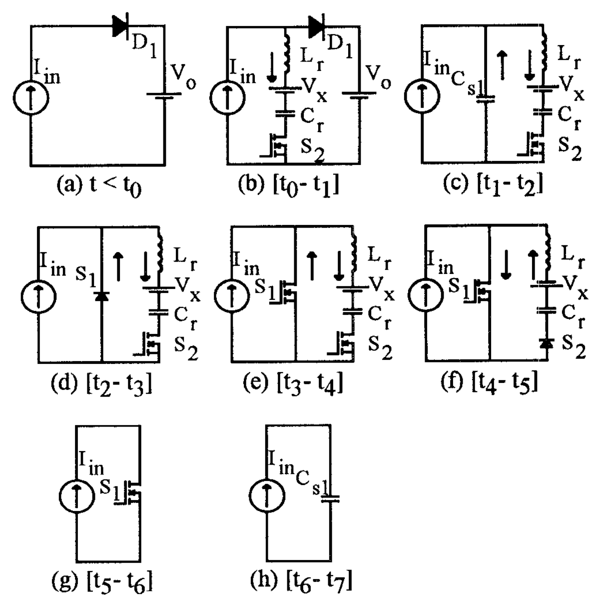

Fig. 3. Modes of operation of the proposed converter.

At the end of the mode, the current flowing through the auxiliary circuit is equal to the input current, and the voltage across the resonant capacitor is V^{**}.

(c) *Mode 2* [t_1- t_2]: Current has stopped flowing through diode D_1 as the current flowing through the auxiliary circuit, I_{Lr}, is greater than the input current. As I_{Lr} continues to rise, the current that exceeds the input current discharges the capacitor across S_1, C_{s1}. The state equations are:

$$L_r \frac{dI_{Lr}}{dt} = V_{Cs1} - V_x - \frac{1}{C_r}\int_0^t I_{Lr}\, dt - V^{**} - I_{Lr}R_r \qquad (9)$$

$$C_r \frac{dV_{Cr}}{dt} = I_{Lr} \quad (10) \qquad C_{s1}\frac{dV_{Cs1}}{dt} = -(I_{Lr} - I_{in}). \quad (11)$$

Using the initial conditions $I_{Lr} = I_{in}$, $V_{Cr} = V^{**}$, and $V_{Cs1} = V_o$, equ. (9) - (11) can be solved to give:

$$I_{Lr} = e^{-\xi t}(A\cos\omega_r' t + B\sin\omega_r' t) + I_{in}\frac{C_p}{C_{s1}} \qquad (12)$$

$$V_{Cs1} = e^{-\xi t}\left(\frac{E}{C_{s1}}\cos\omega_r' t + \frac{F}{C_{s1}}\sin\omega_r' t\right) + I_{in}\frac{C_{s1} - C_p}{C_{s1}^2}t + V_o - \frac{E}{C_{s1}} \qquad (13)$$

$$V_{Cr} = -e^{-\xi t}\left(\frac{E}{C_r}\cos\omega_r' t + \frac{F}{C_r}\sin\omega_r' t\right) + I_{in}\frac{C_p}{C_r C_{s1}}t + V^{**} + \frac{E}{C_r} \qquad (14)$$

where

$$C_p = \frac{C_r C_{s1}}{C_r + C_{s1}} \quad (15) \qquad A = I_{in}\frac{C_p}{C_r} \quad (16)$$

$$B = \frac{V_o - V_x - V^{**} - I_{in}R_r + L_r\xi A}{\omega_r' L_r} \qquad (17)$$

$$E = \frac{\xi A + B\omega_r'}{\omega_o'^2} \quad (18) \qquad F = \frac{\xi B - A\omega_r'}{\omega_o'^2}. \quad (19)$$

Note that ω_o' and ω_r' can be found by substituting C_p for C_r in equ. (6) and (7). This mode ends when C_{s1} has been fully discharged. When this happens, the current flowing through the auxiliary circuit is equal to I^{***}, and the voltage across the resonant capacitor is V^{***}.

(d) Mode 3 [t_2- t_3]: During this time, the anti-parallel diode of S_1 is conducting, and the switch is turned on under ZVS conditions. The state equations are:

$$L_r \frac{dI_{Lr}}{dt} = -\left(V_x + \frac{1}{C_r}\int_0^t I_{Lr}\, dt + V^{****} + I_{Lr}R_r\right) \qquad (20)$$

$$C_r \frac{dV_{Cr}}{dt} = I_{Lr}. \qquad (21)$$

Using the initial conditions $I_{Lr}=I^{***}$ and $V_{Cr}=V^{***}$, equ. (20)-(21) can be solved to give:

$$I_{Lr} = e^{-\xi t}\left(I^{***}\cos\omega_r t - \frac{G + L_r\xi I^{***}}{\omega_r L_r}\sin\omega_r t\right) \qquad (22)$$

$$V_{Cr} = e^{-\xi t}\left(G\cos\omega_r t + \frac{\xi C_r G + I^{***}}{\omega_r C_r}\sin\omega_r t\right) - V_x \qquad (23)$$

where

$$G = V^{***} + V_x. \qquad (24)$$

At the end of the mode, the current flowing through the auxiliary circuit is the same as the input current.

(e) *Mode 4* [t_3- t_4]: Current flows through S_1 as the current flowing through the auxiliary circuit is still positive, but less than the input current. The equations for this mode are the same as those for Mode 3. This mode ends when current I_{Lr} is zero.

(f) *Mode 5* [t_4- t_5]: Current is flowing through the main switch S_1. This current, however, is now the sum of the input current and the current flowing through the auxiliary circuit, through the body diode of S_2. The auxiliary switch S_2 is turned off under ZVS conditions. The state equations are:

$$L_r \frac{dI_{Lr}}{dt} = V_x - \frac{1}{C_r}\int_0^t I_{Lr}\, dt - V^{****} \qquad (25)$$

$$C_r \frac{dV_{Cr}}{dt} = I_{Lr}. \qquad (26)$$

Using the initial conditions are $I_{Lr}= 0$ and $V_{Cr}=V^{****}$, equ. (25)-(26) can be solved to give:

$$I_{Lr} = -\frac{V^{****} - V_x}{\omega_o L_r}\sin\omega_o t \qquad (27)$$

$$V_{Cr} = (V^{****} - V_x)\cos\omega_o t + V_x. \qquad (28)$$

Note that under steady-state conditions, the value of V_{Cr} after this mode is the same as it was before the auxiliary circuit was fired, $V_{Cr} = V^*$.

Converter operation during Modes 6-7 (Figs. 3(g)-(h)) is identical to that of the standard PWM boost converter.

III. Design Guidelines

A. Characterisitc Curves

The equations for the modes of operation that were derived in the previous section can be used to generate characteristic curves that form the basis of a design procedure. Several characteristic curves are shown in Figs. 4 and 5. Although these equations were derived for the case where the input voltage source is dc, they can also be used to determine worst case operating conditions for the converter operating with PFC because an ac input source can be considered can be considered to be dc during a very short switching cycle. Since the auxiliary circuit is activated just before the main switch is turned on, the operation of the circuit is dependent on the input current value at that instant, I_{in}^*, and the output voltage V_o. The curves have thus been generated with respect to the ratio:

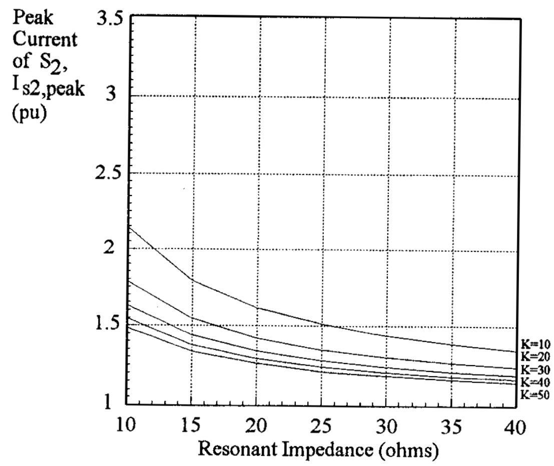

(a) Peak current of S_2, $I_{s2,peak}$, vs resonant impedance, Z_r.

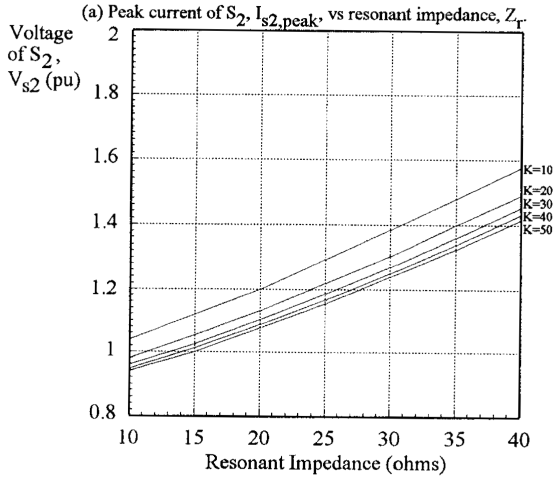

(b) Voltage of S_2, V_{s2}, vs resonant impedance, Z_r.

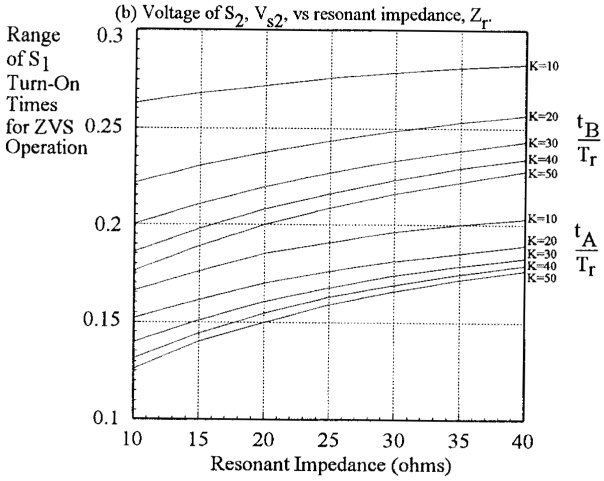

(c) Range of ZVS for S_1 vs. resonant impedance, Z_r.

Fig. 4. Characteristic curves for output voltage / input current ratio $Z_{rb} = 50\ \Omega$ and transformer turns ratio N = 6.

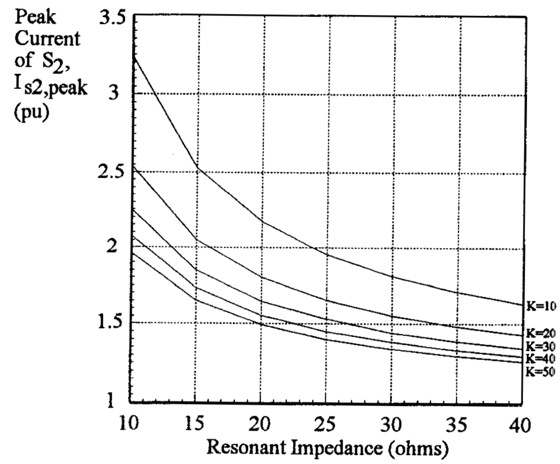

(a) Peak current of S_2, $I_{s2,peak}$, vs resonant impedance, Z_r.

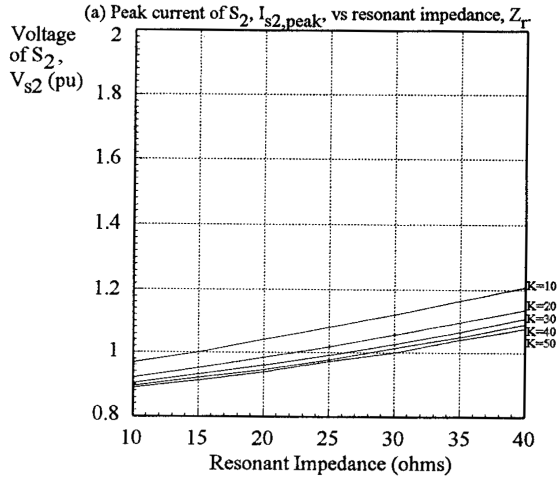

(b) Voltage of S_2, V_{s2}, vs resonant impedance, Z_r.

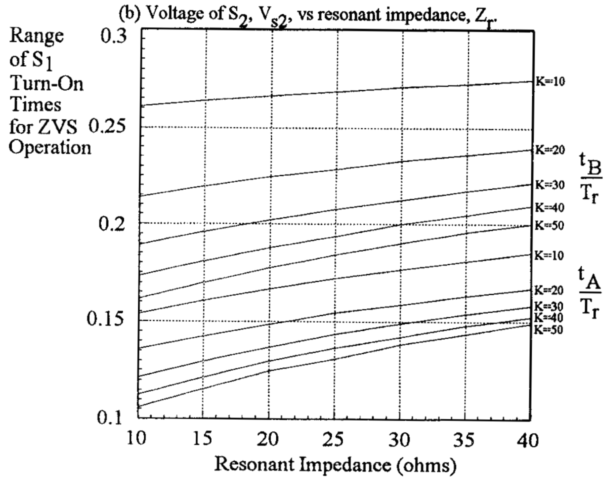

(c) Range of ZVS for S_1 vs. resonant impedance, Z_r.

Fig. 5. Characteristic curves for output voltage / input current ratio $Z_{rb} = 100\ \Omega$ and transformer turns ratio N = 6.

$$Z_{rb} = \frac{V_o}{I_{in}^*}. \tag{29}$$

Figs. 4 and 5 show curves derived for two output voltage / input current ratios: Z_{rb} = 50 Ω and Z_{rb} = 100 Ω. Since the base values for voltage and current are the V_o and I_{in}^* for each operating point, the input current when Z_{rb} = 100 Ω is half that when Z_{rb} = 50 Ω if the output voltage is the same in both cases.

Figs. 4(a) and 5(a) show the relationship between the peak current of the auxiliary switch $I_{s2,peak}$ and the impedance of the auxiliary resonant components

$$Z_r = \sqrt{\frac{L_r}{C_r}} \tag{30}$$

for various values of $K = C_r / C_{s1}$. It can be seen that $I_{s2,peak}$ decreases as Z_r and K increase. It should be noted that peak per unit current values for Z_r =100 Ω in Fig. 5(a) are actually larger than those for Z_r = 50 Ω in Fig. 4(a) even though the actual current is less. High $I_{s1,peak}$ and $I_{s2,peak}$ per unit values occur when Z_{rb} is large because there is current flowing in the auxiliary circuit even when the input current is very small.

Figs. 4(b) and 5(b) show the relationship between the voltage across the auxiliary switch, V_{s2}, and Z_r for various values of $K = C_r / C_{s1}$. It can be seen that V_{s2} increases as Z_r increases and K decreases, and that this voltage is generally greater than V_o which is 1 pu. The excess voltage is due to the negative voltage that exists across C_r when the auxiliary circuit is inactive, but there are operating points where V_{Cr} is actually positive and V_{s2} is less than 1 pu - especially for low values of Z_r.

B. Selection of Main Switch S_1

The voltage and current stresses of the boost switch will be the same as those for the switch in the conventional PWM converter except for the peak current. This will not be more than 2 pu. for the range of operating points shown in Figs. 4 and 5.

C. Selection of Auxiliary Switch S_2

The power rating of the auxiliary switch S_2 is considerably lower than that of the main switch S_1 because it handles very little power as it is on for only a small fraction of the switching cycle. This allows the use of a device that is smaller and less costly than the main switch to be used, but note that the peak current of S_2 is higher than the input current, and the voltage across S_2 is generally higher than it is for S_1 as can be seen in Figs. 4 and 5. The rms value of the current flowing through S_2, $I_{s2,rms}$, can be approximated by equ. (31) by considering it to be a square wave

$$I_{s2,rms} \approx I_{s2,peak} \sqrt{0.4\, T_r f_{sw}}\,. \tag{31}$$

Since current must flow through the body diode of the auxiliary switch which typically has a very slow recovery, it is recommended that the diode be blocked by placing a diode in series with it and a fast recovery diode in parallel with the series diode-switch combination. The ratings for the two diodes are the same as for the auxiliary switch.

D. Selection of Resonant Inductor L_r, Resonant Capacitor C_r and Boost Diode

As was mentioned in the Introduction, one of the problems of the boost converter is the reverse recovery characteristic of the boost diode. This is partially a function of the diode's turn-off di/dt, and can be improved if the current flowing through it is slowly diverted during a controlled rise time after turning on S_2. This rise time is dependent on the value of inductor L_r. The larger the value of L_r, the less recovery current there will be but there will also be more auxiliary circuit conduction losses as the length of the resonant cycle, defined as

$$T_r = 2\pi\sqrt{L_r C_r}\,, \tag{32}$$

and thus the auxiliary circuit rms current are increased. In order to minimize the amount of reverse recovery current while keeping L_r as small as possible, L_r can be designed so that the auxiliary circuit current is allowed to ramp up to within three times the boost diode's specified reverse recovery time, t_{rr}, as suggested in [4]. The value of L_r can be calculated for the proposed converter by using the following equation:

$$L_r = \frac{3 t_{rr} V_{s2}}{I_{in,\max}}. \tag{33}$$

The value of C_r should be selected to be as low as possible to keep the length of the resonant cycle T_r small. If, however, the value of C_r is too low, then this will result in excessive values of $I_{s2,peak}$ and, more importantly, V_{s2}. As a compromise, the value of C_r should be selected so that it is small, but does not allow V_{s2} to exceed some specified limit.

The voltage and current stress of the boost diode are the same as those found in a standard PWM boost converter. This diode should be a fast recovery diode because a slower diode would require a larger value of L_r which would increase the duration of auxiliary circuit operation and conduction losses.

E. Selection of Transformer Turns Ratio and Diodes

When the auxiliary circuit is operating, the voltage across the primary of T_x is clamped to a voltage of $V_x = V_o / N$ where N is the turns ratio. Since the polarity of V_x is set to be opposite that of V_{Cr}, the voltage across L_r and thus the current flowing in the auxiliary circuit I_{Lr} is reduced. The higher the value of V_x, the lower I_{Lr} is, but switch S_1 will not turn on with ZVS if V_x is set to too large a value as there will not be sufficient energy to discharge capacitor C_{s1}. The criterion that is used to select a value of N and thus a value of V_x is therefore that N must be set at the minimum value at which S_1 can be turned on with ZVS. Analysis and experimental work has shown this value to be approximately 6 - 7 for Z_{rb} >= 50 Ω.

The maximum voltage that a transformer secondary diode experiences is twice the output voltage when the other diode is conducting current. The peak and rms values of these diode can be found by dividing the peak and rms values of the auxiliary current by the transformer turns ratio N.

F. Time Interval for ZVS Turn-On of Main Switch S_1.

The main switch of the proposed converter will have a ZVS turn-on only if it is turned on after capacitor C_{s1} has been discharged at time $t = t_A$, but before the current through the resonant circuit drops below the input current at $t = t_B$, thus recharging C_{s1}. This means that a ZVS turn-on will occur as long as S_1 is turned on at a time instant within the time interval t_A - t_B ($t = t_0$*), after the auxiliary switch S_2 has been turned on at time t_0, as shown in Fig. 6. Fig 4(c) and 5(c) show times, t_A and t_B, defined with respect to the resonant cycle of the auxiliary circuit, T_r for Z_{rb} = 50 Ω and Z_{rb} = 100 Ω respectively. A ZVS turn-on for S_1 will be guaranteed if $t = t_0$* is set so that it is between the t_A and t_B curves for the minimum value of Z_{rb} that will be encountered during converter operation.

IV. Design Procedure and Example

The following example is given to demonstrate the design procedure used to determine the values of the auxiliary circuit components, and the ZVS time interval t_A-t_B. The converter is to be designed with output power: P_o = 600 W, output voltage: V_o = 300 Vdc, input voltage: V_{in} = 100 - 250 Vdc, switching frequency f_{sw} = 50 kHz. It is assumed that the input inductor is large enough so that the input current has little ripple, that a value of C_{s1} = 1 nF is sufficient to minimize S_1 turn-off losses, and that the boost diode has a reverse recovery time of t_{rr} = 60 ns. It is also assumed, as an initial estimate, that converter efficiency is η >= 95%. The values are to be selected so that the voltage across the auxiliary switch, V_{s2}, does not exceed 1.25 pu. A transformer turns ratio of N = 6 will be used.

(1) Determine the value of $Z_{rb} = V_o / I_{in}^*$ where the input current is at its peak. The peak switch voltages and currents occur at this point. The input current is at its maximum value when V_{in} = 100 V and is

$$I_{in,\max} = \frac{P_o}{V_{in}\,\eta} = \frac{600}{100 \cdot 0.95} = 6.3A. \qquad (34)$$

The minimum value of Z_{rb} is $Z_{rb,min}$ = 300 / 6.3 = 47.5 Ω. The curves in Fig. 4 which are for Z_{rb} = 50 Ω will be used in this example.

(2) Use equ. (33) to determine the value of L_r:

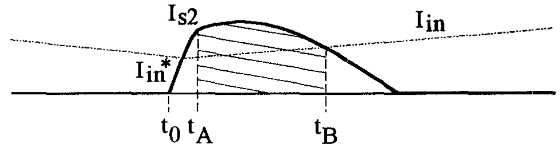

Fig. 6. Time interval during which S_1 should be turned on for ZVS turn-on.

$$L_r = \frac{3(60ns)(1.25 \cdot 300V)}{6.3A} = 10.6\mu H. \qquad (35)$$

(3) Using Fig. 4(b) find the smallest value of C_r so that V_{s2} <= 1.25 pu. This can be approximated to be C_r = 17 nF at Z_r = 25 Ω and K = 17. V_{s2} = 1.25 V x 300 pu = 375 V.

(4) Using K and Z_r, find $I_{s2,peak}$ from Fig. 4(a). For K = 17 and Z_r = 25 Ω, $I_{s1,peak}$ ≈ 6.3 A x 1.4 pu = 8.8 A.

(5) Calculate the value of T_r using equ. (32)

$$T_r = 2\pi\sqrt{10.6\,\mu H \cdot 17nF} = 2.67\,\mu s \qquad (36)$$

then find the values of t_A and t_B from Fig. 4(c) for K = 17 and Z_r = 25 Ω: t_A = 0.18 x 2.67 μs = 480 ns and t_B = 0.25 x 2.67 μs = 670 ns. Since the ZVS interval is at its narrowest when $Z_{rb} = Z_{rb,min}$, S_1 will be guaranteed to have a ZVS turn-on for higher values of Z_{rb}.

(6) Set the pulsewidth of the gating signal of S_2 to be more than 0.6 T_r = 1.6 μs but less than 0.9 T_r = 2.4 μs.

(7) Calculate the rms value of the auxiliary switch current using equ. (31)

$$I_{s2,rms} \approx 8.8A\,\sqrt{0.4(2.67\mu s)(50kHz)} = 2.0A. \qquad (37)$$

(8) The peak voltage stress across the transformer diodes is 2 pu or 2 x 300 V = 600 V. The peak current and rms current are Is2,peak / 6 = 1.47 A and Is2,rms / 6 = 0.33 A.

V. Experimental Results

The feasibility of the proposed converter was verified with results obtained from an experimental prototype. Fig. 7(a) shows the voltage across the main switch S_1, and the combined current through S_1, its body diode, and capacitor C_{s1}. It can be seen that the negative current, which caused by the operation of the auxiliary circuit, completely discharges C_{s1}, ensuring a ZVS turn-on. Fig 7(b) shows the same pair of waveforms on a different time scale. Although the voltage across the switch is the same as the switch voltage found in a standard PWM boost converter, the current does have a slight resonant peak. Fig 7(c) shows the current flowing through the boost diode. Note that there is no reverse recovery current due to the operation of the auxiliary circuit. Fig. 8 shows the efficiency of the proposed converter as a function of input voltage compared with that of a conventional PWM converter. It can be seen that the proposed converter has a significantly better efficiency than the PWM converter, especially for low line conditions.

VI. Conclusion

A ZVS PWM boost converter was proposed in this paper. The features of this converter include PWM control with soft-switching over a wide line and load range for all active and passive switches and low peak switch stresses due to a simple energy feedforward auxiliary circuit. The modes of operation were explained and analyzed in detail. The results of the analysis were used to generate characteristic curves which were used to develop guidelines for the design of converter components and for ZVS operation. The feasibility of the proposed converter was verified experimentally on a 600 W prototype.

References

[1] G. Hua, C-S Lieu, Y. Jiang, and F. C. Lee, "Novel zero-voltage-transition PWM converters," *IEEE Trans. on Power Elec.*, vol. 9, no. 2, pp. 213-219, Mar. 1994.

[2] L. Yang and C. Q. Lee, "Analysis and design of boost zero-voltage-transition PWM converter," in *IEEE Appl. Power Elec. Conf. Rec.*, 1993, pp. 707-713.

[3] J. P. Gegner and C. Q. Lee, "Zero-voltage-transition converters using a simple magnetic feedback technique," in *IEEE Appl. Power Elec. Conf. Rec.*, 1994, pp. 590-596.

[4] J. Bazinet and J. O'Connor, "Analysis and design of a zero-voltage-transition power factor correction circuit," in *IEEE Appl. Power Elec. Conf. Rec.*, 1994, pp. 591-600.

[5] G. Moschopoulos, P. Jain and G. Joos, "A novel zero-voltage switched PWM boost converter," in *IEEE Power Elec. Spec. Conf. Rec.*, 1995, pp. 694-700.

[6] K. M. Smith and K. M. Smedley, "A comparison of voltage mode soft switching methods for PWM converters," in *IEEE Appl. Power Elec. Conf. Rec.*, 1996, pp. 291-298.

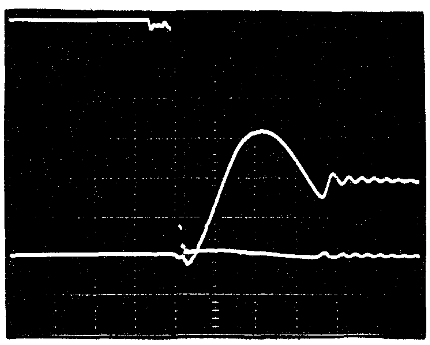

(a)

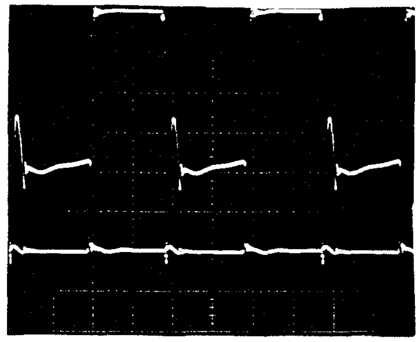

(b)

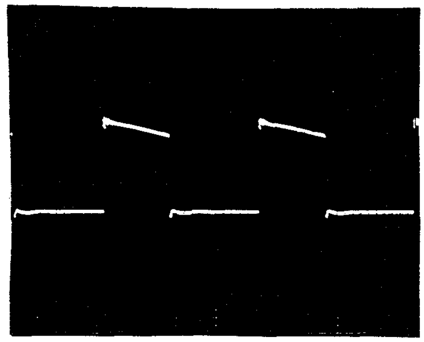

(c)

Fig 7. Experimental results. (a) Main switch S_1 turn-on (V: 50 V/div., I: 2 A/div., t: 500 ns/div.). (b) Main switch S_1 waveforms (V: 100 V/div., I: 2 A/div., t: 5 µs/div.). (c) Boost diode current (V: 100 V/div., I: 2 A/div., t: 5 µs/div.).

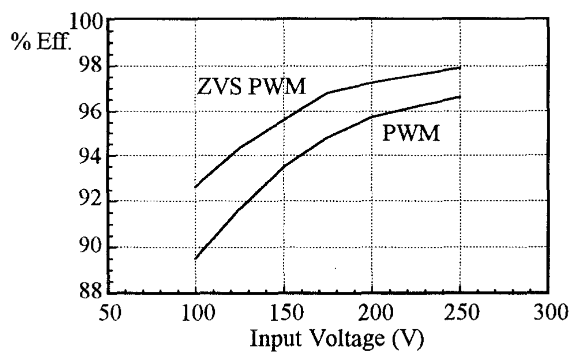

Fig. 8. Measured % efficiency vs. input voltage.